Oxidation of Metals, Vol. 40, Nos. 3/4, 1993

Simultaneous Chromizing–Aluminizing Coating of Low-Alloy Steels by a Halide-Activated, Pack-Cementation Process

Frederick D. Geib*† and Robert A. Rapp*

Received November 6, 1992; revised April 6, 1993

The simultaneous chromizing–aluminizing of low-alloy steels has achieved Kanthal-like surface compositions of 16–21Cr and 5–8 wt.% Al by the use of cementation packs with a Cr–Al masteralloy and an NH_4Cl activator salt. An initial preferential deposition of Al into the alloy induces the phase transformation from austenite to ferrite at the 1150°C process temperature. The low solubility of carbon in ferrite results in the rejection of solute C into the austenitic core, thereby preventing the formation of an external Cr-carbide layer, which would otherwise block aluminizing and chromizing. The deposition and rapid diffusion of Cr and Al into the external bcc ferrite layer follows. Parabolic, cyclic-oxidation kinetics for alumina growth on the coated steels in air were observed over a wide range of relatively low temperatures (637–923°C).

KEY WORDS: Cr–Al coating; pack cementation; cyclic oxidation; isothermal scaling.

INTRODUCTION

Steel remains the material of choice for numerous applications largely because of its low cost and the wide variety of properties available through alloy design, heat treatment, and mechanical-forming techniques. However, alloy steels with adequate high-temperature strength, such as those used in

*Department of Materials Science and Engineering, The Ohio State University, Columbus, Ohio 43210.
†Current address: The Timken Company, RES-13, 1835 Dueber Ave., S.W., Canton, Ohio 44706-6930.

0030-770X/93/1000-0213$07.00/0

petrochemical or electric-utility plants, etc. at 550–800°C often have poor oxidation, sulfidation and hot-corrosion resistance.[1] The need for improved processing efficiency for these systems often requires higher service temperatures for alloys. Although Fe–Cr alloys with $N_{Cr} > 0.20$ often possess adequate oxidation resistance owing to the formation of a protective chromia scale, their use is limited by high cost and inadequate mechanical properties. The protection of steels by a slow-growing alumina scale is superior in any case, especially in resisting attack by mixed oxidants. However, steels alloyed with sufficient Al ($N_{Al} > 0.10$) to form a protective, external alumina scale would have poor ductility and fracture toughness,[2] and have no practical importance.

The beneficial synergistic interaction of Cr and Al to provide excellent oxidation resistance for steels has been exploited in the well-known iron-base Kanthal alloy which contains about 20 wt.% Cr and 5 wt.% Al. According to Wagner's secondary-getter mechanism,[3] during the oxidation of such an alloy, the rapid oxidation of Fe and the internal oxidation of Al are prevented by the formation of an initial transient thin chromia scale. This gettering of oxygen by chromia results in a very low oxygen activity at the alloy/scale interface and thus allows Al to reach the interface by diffusion to form (in the steady state) a slow-growing, thermodynamically more stable Al_2O_3 scale, which is an effective barrier to the inward diffusion of the oxidant and the outward diffusion of cations.[3] However, for the bulk Kanthal alloy, this excellent corrosion resistance is achieved at the expense of mechanical properties, since the alloy has low ductility at room temperature and low strength at elevated temperatures.

To take advantage of the low cost, good mechanical properties, and fabricability of alloy steels, various corrosion-resistant coatings are commonly deposited commercially. Among these methods, the *in situ* CVD process known as pack cementation has the advantages of low cost and applicability to various shapes and sizes. The pack-cementation process involves placing the parts to be coated in a reactive pack of powders, and heating this pack in a vented retort to an elevated temperature (e.g., 1000–1150°C) for a given period of time (e.g., 4–16 hr) during which a diffusion coating is produced. The packs contain the part(s) to be coated, a powder masteralloy (containing the desired element(s) for deposition), a halide-activator salt, and an inert-powder filler (e.g., Al_2O_3). An inert carrier gas fills and surrounds the pack. At the process temperature, the activator salt reacts with the elements of the masteralloy to form metallic halide vapors which diffuse through the gas phase of the porous pack to the substrate where deposition and solid-state diffusion occur. The gaseous and solid-state diffusion steps are rate-limiting, and the gas phase of the

pack far from the substrate may be modeled as a closed system in thermodynamic equilibrium.[4]

Steels have been coated commericially by the pack-cementation process to deposit either Cr or else Al, or both in a sequential manner, to produce surface compositions which exhibit improved resistance to high-temperature corrosion. Although the feasibility for simultaneous codeposition of Cr with Al has been questioned on thermodynamic grounds,[5] codeposited Cr/Al diffusion coatings of nominal 250-μm thickness have been experimentally produced on Fe-base alloys using a Cr–Al alloy powder with low-Al activity and a low-stability chloride activator salt.[6–8] A discussion of the thermodynamic problem involved in achieving codeposition of Cr and Al, and the route required for its resolution, have been presented by Kung and Rapp.[9] Despite some previous advances toward Cr/Al codeposition, reproducible surface compositions on steels containing carbon have been elusive since the Cr-rich masteralloys used have commonly led to the formation of a surface Cr-carbide which excludes the deposition of Al.[10]

Thermodynamics

For the simultaneous chromizing/aluminizing of low-alloy carbon steels, the partial pressures of Cr-halides and Al-halides in the pack must be comparable and of a significant magnitude. This is only possible when the thermodynamic activity of Al in the pack is reduced to 2–3 orders of magnitude below that for Cr.[9] The Al–Cr phase diagram of Fig. 1, and the Cr and Al activity plots of Fig. 2[4] provide the necessary information. The corresponding Cr–Al masteralloy composition required for Cr–Al codeposition has been shown in recent studies to be at least 90 wt.% Cr (balance Al).[10] Since these masteralloys are single phase Cr–Al solid solutions, the activity of the masteralloy element which is preferentially deposited must decrease during the process. For simultaneous chromizing/aluminizing, an initial deposition and diffusion of Al is essential to avoid Cr-carbide formation at the surface.

When the surface composition of a steel substrate at 1150°C reaches a level greater than 1 wt.% Al, the phase transformation from austenite to ferrite occurs. Chromium, also a ferrite stabilizer, must reach a surface concentration greater than 12 wt.% to induce the same transformation at 1150°C. But, as is common for chromizing steels, chromium carbide ($Cr_{23}C_6$) forms as a surface layer by the rapid outward diffusion of chromium. This surface carbide blocks the inward diffusion of Al and locally depletes the steel of carbon needed for strength. Since the Al activity (and thus the Al-halide partial pressures) is difficult to control using

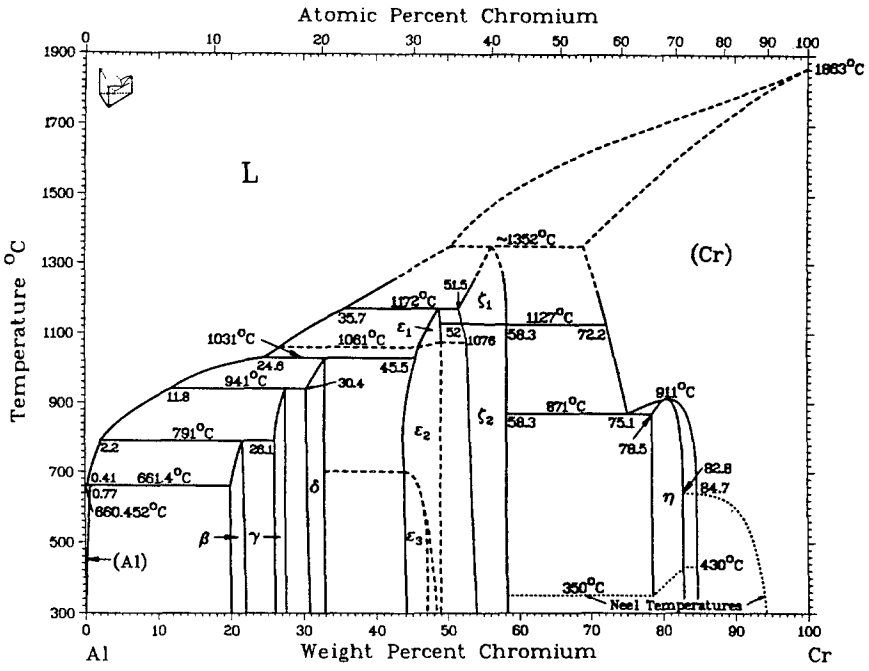

Fig. 1. Phase diagram for the Al–Cr system.[11]

single-phase Cr–Al masteralloys, the flux of Al to the substrate must be controlled in another way. The Al deposition is supported by Al-halide, partial pressure gradients set up near the substrate/pack interface. Halide partial pressures in the bulk pack (away from the substrate) were calculated by Bianco and Rapp[12] (using ITSOL[10,13]) for low-Al, high-Cr masteralloys in NH_4Cl-activated packs as shown in Fig. 3. These calculations demonstrate the condition needed for simultaneous chromizing/aluminizing (i.e., comparable and significant partial pressures for the relevant Cr and Al halides).

To codeposit first Al and then Cr plus Al, an effective control of the Al flux to the substrate can be achieved in packs in which a relatively low amount of Cr–Al masteralloy is used. A wider masteralloy-depletion zone develops at the pack/substrate interface in these "lean" packs, which leads to a smaller Al-halide partial pressure gradient and a lower Al flux to the substrate. In the research described here, an NH_4Cl-activated "lean" pack process, in which a low amount of 90Cr–10 wt.% Al masteralloy powder is used, has reproducibly yielded coating surface compositions of 16–21Cr and 5–8 Al. The Cr/Al coatings produced by this modified process have

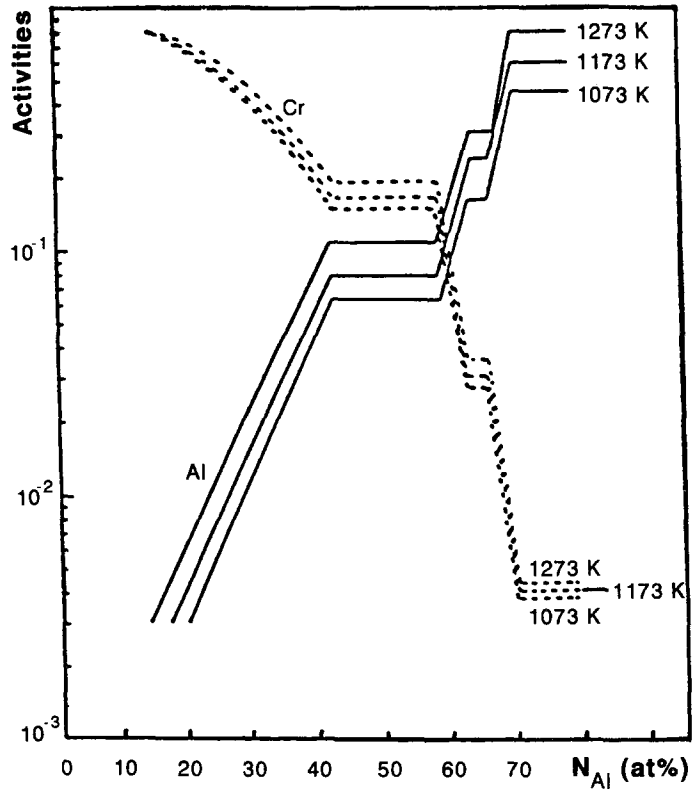

Fig. 2. Aluminum activity vs. at.% Al for the Cr–Al system.[4]

been characterized in terms of their microstructure and composition profiles, and their cyclic-oxidation behavior.

EXPERIMENTAL PROCEDURES

The two boiler steels used in this study had compositions of Fe–2.25Cr–1.0Mo–0.15C and Fe–0.5Cr–0.5Mo–0.1C and were supplied by Babcock & Wilcox Co. Masteralloys with compositions of 90Cr–10 wt.% Al, 92Cr–8Al, and 92.5Cr–7.5Al were purchased as −100 mesh powder from Consolidated Astronautics, Inc. The $AlCl_3$ and NH_4Cl activator salts were certified reagent grade.

The pack mixtures for the chromizing-aluminizing of these steels consisted of 2 wt.% activator, 5–25% masteralloy and 93 to 73% alumina powder (80–200 mesh). The alumina filler powder prevents sintering of the

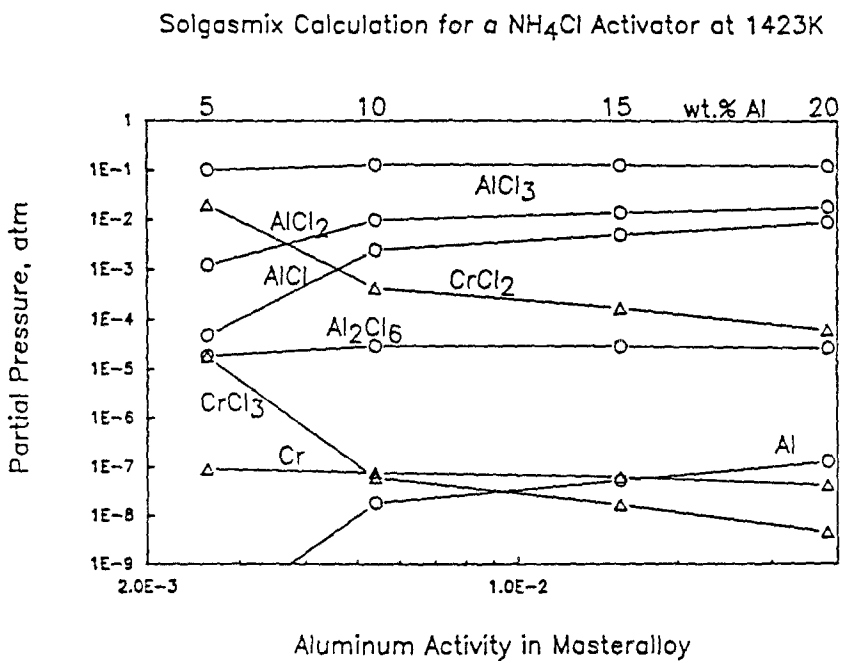

Fig. 3. Equilibrium partial pressures of gaseous species vs. aluminum activity in a NH_4Cl-activated pack at 1423 K for Cr–Al masteralloys.[12]

masteralloy and allows diffusion of the vapor species. Coupons of about $1.0 \times 0.5 \times 0.2$ cm were ground to 600-grit SiC paper. The initial dimensions and mass were recorded, and each coupon was ultrasonically cleaned before processing.

In these laboratory studies, the specimens and powder blend were loaded into an alumina crucible, which was closed with an alumina disc sealed with Cerambond alumina cement (Aremco Products, Inc.). The sealed retort was cured for 24 hr at room temperature and then placed horizontally inside an alumina reaction tube in a resistively-heated furnace. A purification train was used to remove moisture, carbon dioxide, and oxygen from the argon supply. When the furnace temperature reached approximately 500°C, the pack was pushed by a thermocouple into the furnace hot zone. The argon flow was maintained around the pack to prevent oxidation of the substrates and the masteralloy. Process temperatures ranged from 1050 to 1150°C for 4–16 hr. Upon completion of the process, the coated coupons were ultrasonically cleaned, and the final dimensions and mass were recorded. The coupons were sectioned and prepared for metallography. The chromized-aluminized steel coupons were

etched with a 50–50 nitric acid/methanol solution; high-Cr coatings did not etch easily.

Each coating process was evaluated in terms of the microstructure, composition, and thickness of the coatings produced. Accordingly, adjustments were made to the pack compositions and/or process parameters for succeeding runs. A JEOL JSM-820 scanning electron microscope (SEM) was operated at 20 kV and used with a Noran EDS system to determine concentration profiles through coating cross-sections. Analyses for the light elements C, N, and O were performed using a fully automated Cameca SX–50 microprobe (using wavelength-dispersive spectroscopy, WDS) operated at 15 kV and 20 nA, with 1–5 μm beam size.

RESULTS AND DISCUSSION

Coating Results

A previous Cr/Al coating study by Miller[10] is summarized in the top part of Table I along with initial results of the current study (bottom part of Table I). As indicated by Miller's results in the top of Table I, the

Table I. Surface Compositions of Coatings for Various Simultaneous Cr/Al Coating Process Conditions

Masteralloy	Activator	Time/temp.	Surface comp.
Packs of 25 wt.% masteralloy[10]			
92Cr–8Al	NaCl	25 hr/1000°C	Fe–11Al–6Cr
92.5Cr–7.5Al	NaBr	24 hr/1050°C	Fe–5Al–7Cr
92Cr–8Al	$AlCl_3$ + NaBr	16 hr/900°C, then, 8 hr/1150°C	Fe–18Cr–9Al[a]
92.5Cr–7.5Al	$AlCl_3$ + NaBr	16 hr/900°C then, 8 hr/1150°C	Fe–20Cr–3Al
Wt.% M.A.	Activator	Time/temp.	Surface comp.
Packs of 5–25 wt.% 90Cr–10Al masteralloy (this study)			
25	$AlCl_3$	16 hr/1050°C	Fe–8Cr–17Al
10	$AlCl_3$	16 hr/1050°C	Fe–11Cr–9Al
8	$AlCl_3$	(same)	Fe–14Cr–6Al
8	NH_4Cl	(same)	Fe–13Cr–8Al
8	NH_4Cl	(same)	Fe–14Cr–7Al
7	$AlCl_3$	(same)	Fe–16Cr–5Al
7	NH_4Cl	(same)	Fe–14Cr–7Al
7	NH_4Cl	(same)	Fe–35Cr–0.6Al
5	$AlCl_3$	(same)	Fe–24Cr–0Al

[a]Compositions ranged from 13 to 20Cr and 4 to 9Al.

desired Kanthal-like (15–25Cr, 4–8Al) coating surface compositions were not consistently produced. Indeed, the surface compositions were very sensitive to the Cr activity of the masteralloy when using the unstable activators $AlCl_3$ or NH_4Cl. These previous processes led to either the formation of an external Cr-carbide layer (slightly high a_{Cr}) or else to a low-Cr/high-Al composition (slightly lower a_{Cr}). The process window to achieve the desired surface composition was too narrow to permit reproducible satisfactory results. Figure 4a[10] shows a coating microstructure for which the surface layer was identified as $Cr_{23}C_6$. The associated decarburization of the substrate, as evidenced by the absence of pearlitic microstruc-

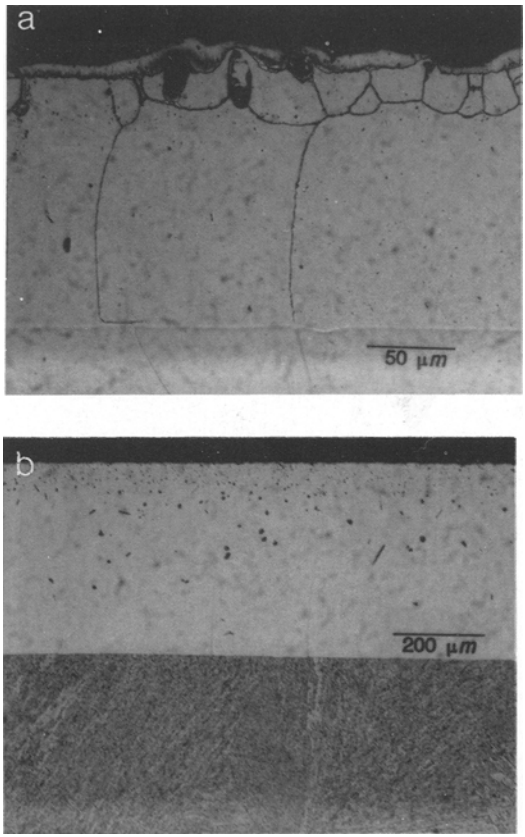

Fig. 4. Cross-sectional optical micrograph of coatings on 2.25Cr–1Mo steel using: (a) 25 wt.% 92.5Cr–7.5Al, and (b) 25 wt.% 90Cr–10Al masteralloy with NH_4Cl activator diffused at 1050°C for 16 hours (Al_2O_3 filler).[10]

ture below the substate/coating interface, is a serious liability to the creep strength of the alloy. Figure 4b[10] shows a microstructure for which the surface composition is 10Cr and 10Al. In this case, at the process temperature, the inward diffusion of Al induced the phase transformation of austenite (fcc) to ferrite (bcc), which has a very low C solubility. Also, since Al must have a highly positive thermodynamic interaction coefficient with C ($\varepsilon_{Al}^{C} = +5.3$ in liquid Fe at 1600°C),[14] Al serves to reject C into the austenitic substrate, which has a much higher C solubility. In Fig. 4b, no surface carbide was present and the substrate was enriched in C (pearlite).

To widen the process window to achieve reproducible Kanthal-like surface compositions (Table I, bottom), a "lean pack" containing a lesser amount of masteralloy was tried. The 90Cr–10 wt.% Al masteralloy is mainly an aluminizer when used with volatile activators such as $AlCl_3$ and HN_4Cl. However, the preferential extraction of aluminum from the masterallow during the process shifts its composition to favor chromizing. But the amount of masteralloy used previously (25%) did not achieve a sufficient local Al depletion to convert the process of chromizing. When the amount of masteralloy in the pack is decreased from 25 wt.% to 10 wt.% or less, the initial aluminization (forming ferrite) prevents the carbon from reaching the surface so that carbide formation is avoided, and the subsequent Cr diffusion into bcc ferrite is much faster than in fcc austenite.[15] Thus, for a lean pack, the width of the masteralloy-depletion zone and the degree of composition change adjacent to the substrate surface are increased. In this way, an initial Al deposition (leading to ferrite formation and local Al depletion) causes the masteralloy near the substrate to shift its composition to permit deposition of the less-favored constituent (Cr). The reverse of this sequence would result in the formation of an undesirable Cr carbide at the surface, which is observed in the current commercial practice for chromizing steels.

The use of lean packs did not immediately lead to satisfactory coatings. A coating produced in a lean pack with 8 wt.% 90Cr–10Al masterallow content for 16 hr at 1050°C showed a ~70-μm porous outer layer and a substantial weight *loss* (~40 mg/cm^2). Upon removal of these coated samples from their pack, a dark layer of masteralloy-depleted pack powder (~1–2 mm thick) was observed to encase the coupons, while the pack farther away was light-colored and undepleted, as shown in Fig. 5. The porous coating resulted from the back (reverse) diffusion of Cr and Al late in the process when Cr- and Al-depletion zones formed in the lean packs. The loss of Fe by $FeCl_2$ evaporation certainly contributed to the high weight losses. Surface compositions for such porous coatings of ~12–16Cr and 5–7Al were consistently achieved using 7–8 wt.% 90Cr–10Al masteralloy in the NH_4Cl- or $AlCl_3$-activated packs (Table I, bottom).

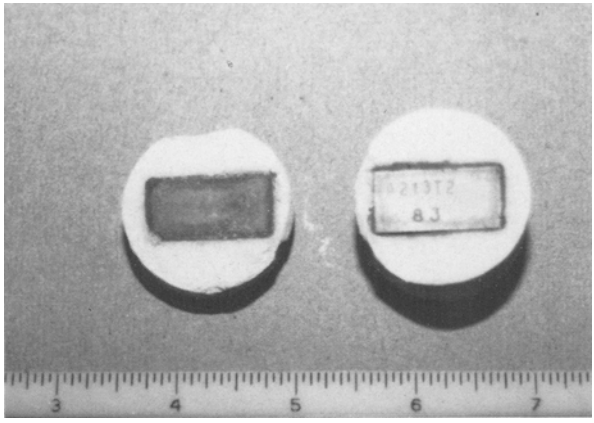

Fig. 5. Photograph of coupon surrounded by depleted pack powder (8 wt.% 90Cr–10Al + NH_4Cl, 6 hr/1150°C). Pack layer shown at left contacted the coated coupon shown at right.

To avoid the development of a porous coating layer, the reverse diffusion of Cr and Al upon pack depletion needed to be minimized. Since coating growth typically follows parabolic kinetics, faster growth occurs during the early part of the process. In lean packs, with more extreme Cr/Al depletion zones adjacent to the substrates, the development of reverse activity gradients must occur during the latter part of the process. Therefore, the processing time was cut from 16 to 6 hr and the temperature was increased from 1050 to 1150°C, to provide faster coating growth. Figure 6 shows the microstructure and concentration profiles for a coating processed at 1150°C for 6 hr. The outer porous layer was not present to the same degree as for the 16 hr/1050°C packs, and the weight-loss was only $\sim 10\ mg/cm^2$. The surface concentration of 12.6Cr–7.7Al was consistent with the results of Table I, bottom, for a 10 wt.% 90Cr–10Al, NH_4Cl-activated pack. The coating thickness of 400 μm (excluding porosity) exceeded the typical industrial requirement[16] of 0.010 inch (254 μm) for coating thickness, so that an even shorter diffusion time at 1150°C seemed preferable.

Coatings were also attempted using 15 wt.% of the 92Cr–8Al master-alloy in order to increase the Cr content to match more closely the Kanthal composition of ~20Cr (with 4.5Al). A 6 hr/1150°C NH_4Cl-activated pack yielded a coating with only a small porous outer layer, but the process was only chromizing, with 35Cr–0.6Al at the coating surface. Decarburization was observed below the coating/substrate interface as evidence for the formulation of a Cr-carbide outer layer which excludes the inward diffusion

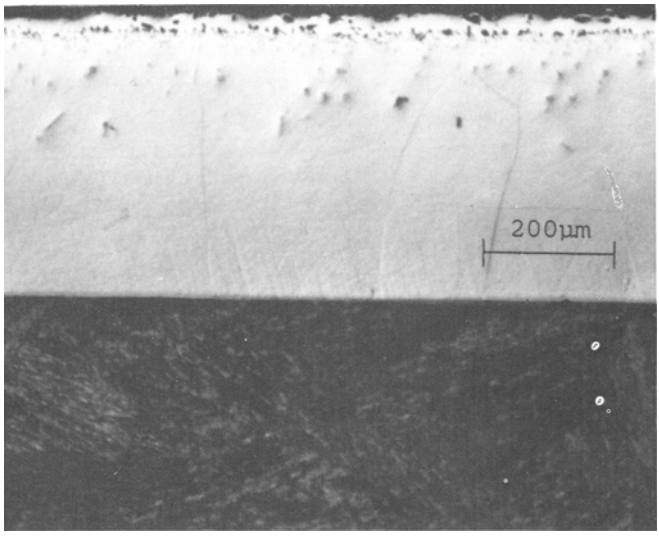

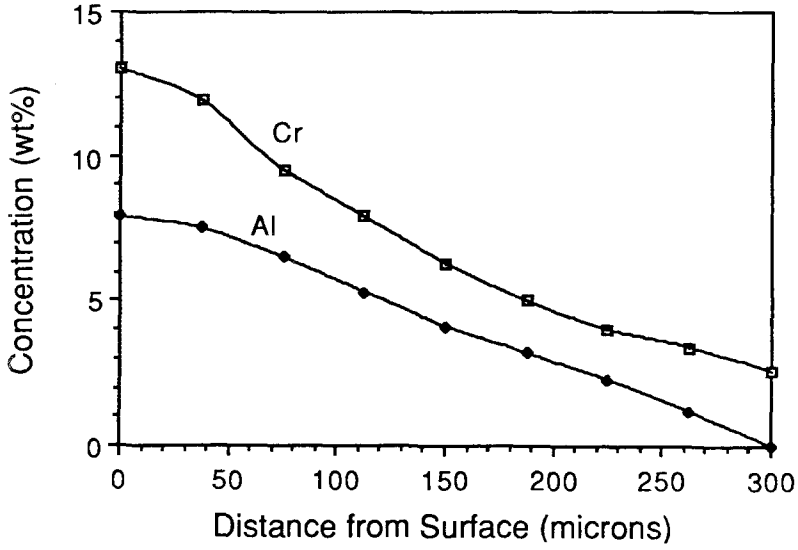

Fig. 6. Microstructure and concentration profiles for coating on 2.25Cr–1Mo steel using 10 wt.% 90Cr–10Al masteralloy and NH_4Cl activator diffused at 1150°C for 6 hours (Al_2O_3 filler).

of Al. At 1150°C, some Cr released by dissociation of the external carbide diffuses into the substrate and precipitates carbide on the grain boundaries.[10] Such a coating is typical for the commercial chromizing process. Therefore, the 92Cr–8Al masteralloy exhibits a Cr activity which is high, and the 90Cr–10Al masteralloy showed the most promise to avoid the surface Cr-carbide layer, while allowing Al to diffuse into the surface.

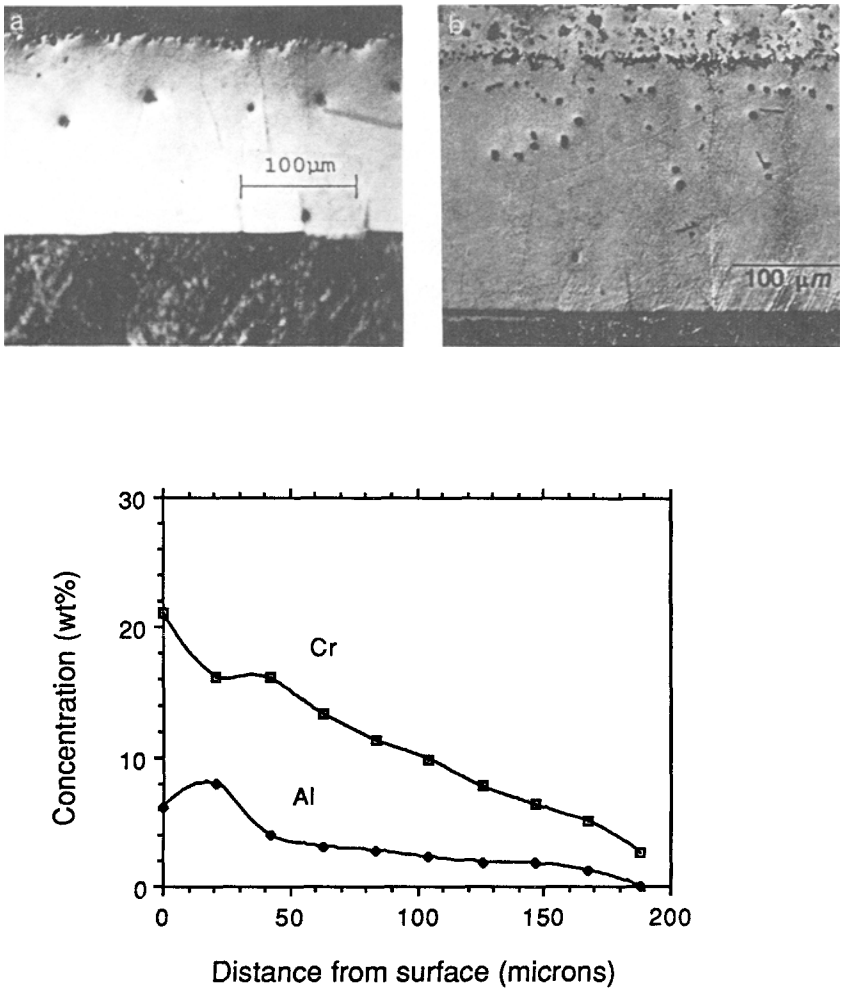

Fig. 7. (a) Microstructure and concentration profiles for coating on 2.25Cr–1Mo steel using 8 wt.% 90Cr–10Al masteralloy and NH_4Cl activator diffused at 1150°C for 4 hr, and (b) 1150°C for 6 hr (Al_2O_3 filler).

A shorter 4 hr/1150°C process using NH_4Cl activator and 8 wt.% 90Cr–10Al masteralloy was tested in an attempt to minimize further the porous outer layer. The resulting microstructure and concentration profiles are shown in Fig. 7a. The process nearly achieved the desired composition for the coating, although beneath the 21Cr–6Al porous outer layer (at 21 μm) the composition changed to 16Cr–8Al, indicating the later preference for Cr deposition. Also, precipitates in the coating layer became more prominant. Spot analysis using a 1-μm WDS probe showed these precipitates to have a composition rich in Al, with negligible amounts of C or O. The NH_4Cl activator was the only source of N for the formation of AlN precipitates. Another pack (Fig. 7b) was processed under the same conditions as that of Fig. 7a, except for 6 hr. With ample coating thickness ($\sim$200 μm) and smaller precipitates in the coating, the microstructure and 19.2Cr–5.0Al surface composition were nearly ideal. These processing conditions have yielded consistently acceptable coatings, in terms of composition, thickness and microstructure, and the formation of Cr-carbide has been avoided. The reversed diffusion fluxes which led to high weight losses and porous coatings were avoided by decreasing the processing time to 4–6 hr and raising the temperature to 1150°C.

Cyclic-Oxidation Results

Cyclic-oxidation tests were conducted in air, and the weight gains are presented in Fig. 8. Coupons were placed on a quartz tray at 1-inch intervals and oxidized simultaneously; a thermocouple monitored the temperature (637–923°C) of each coupon. Slow alumina-scale-growth kinetics were observed for the coatings, even for these relatively low temperatures. Coupons tested above 900°C had consistent values for $\log k_p$ (g^2/cm^4s) of approximately -12 which compares favorably with k_p values found for similar Fe–Cr–Al alloys at only 800°C.[17]

Since the mechanical properties of these steels limit their service temperature, the cyclic oxidation resistance of chromized/aluminized steels at moderate temperatures (in this case, 637–715°C) is most important. Four coatings with surface composition 19Cr–5Al were tested in this lower temperature range. After 444 hr and 11 cycles from test temperature to room temperature, the weight gains were below 0.5 mg/cm^2 (with no spalling detected). Slow steady-state, alumina-growth kinetics were reached for all four coatings at their respective temperatures. From the values for k_p obtained in these tests, a 69 kcal/g-mole activation energy for oxidation was determined from the Arrhenius plot in Fig. 9. This activation energy compares reasonably with the extrapolation of data for higher-temperature tests of bulk alumina-forming alloys,[18,19] although the magnitudes for the

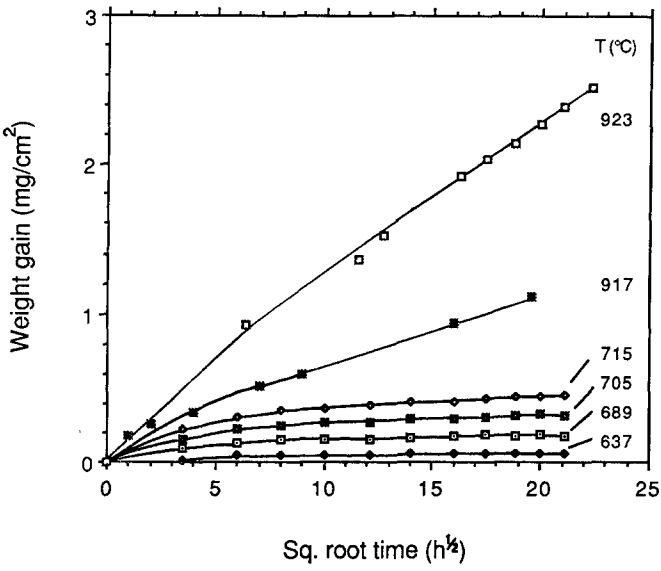

Fig. 8. Cyclic oxidation of Cr/Al coatings in air at 637–923°C. Each indicated point represents a cycle from test temperature to room temperature.

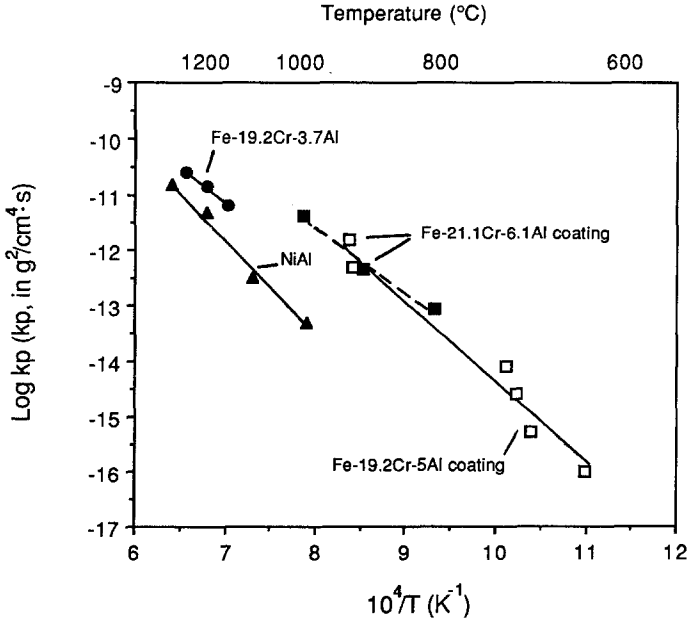

Fig. 9. Arrhenius plot of $\log k_g$ vs. T^{-1} for the oxidation of alumina-forming alloys.[18,19]

rate constants are about a factor of 10 higher than for isothermal oxidation of alloys in the low-temperature regime. An X-ray diffraction pattern for the oxide formed near 900°C shows the presence of alpha alumina. The oxidation kinetics for beta NiAl tested below 1000°C[20] were nearly coincident with those of the Cr–Al coatings in this study.

CONCLUSIONS

A reproducible simultaneous chromizing/aluminizing coating process has been developed for boiler steels using "lean" packs with only 8 wt.% of the 90Cr–10Al masteralloy. Extensive masteralloy depletion adjacent to the substrate allows for the initial deposition of the ferrite-stabilizer, Al, which rejects carbon into the austenitic substrate, thereby preventing the formation of a diffusion-blocking Cr-carbide layer. Thereafter, chromium is able to deposit and diffuse into the ferrite coating layer to provide surface-coating compositions similar to the oxidation-resistant Kanthal alloy. Shorter processing times at a higher temperature (4–6 hr/1150°C) produced sound coating microstructures with the desired composition and adequate coating thicknesses of $\sim 200\ \mu$m. Parabolic cyclic-oxidation kinetics from 637–923°C show an Arrhenius relationship which compares well to higher-temperature data for alumina-forming alloys, NiAl and Fe–19.2Cr–3.7Al. No spalling of the scales was observed.

ACKNOWLEDGMENTS

The authors appreciate the financial support of the Fossil Energy Materials Program of Oak Ridge National Lab (Dr. Rod Judkins, monitor) on project 19XSB154C. The earlier studies of Drs. D. M. Miller and P. A. Choquet led to the prospect for the effective chromizing/aluminizing reported here.

REFERENCES

1. W. T. Bakker and R. A. Perkins, Proc. 3rd Berkely Conf. on Corrosion/Erosion/Wear of Materials at Elevated Temperatures, Jan. (1990).
2. C. S. Giggins and F. S. Pettit, *Met. Trans.* (1970).
3. C. Wagner, *Corros. Sci.* **5**, 751–764 (1965).
4. B. Nciri and L. Vandenbulke, *J. Less-Common Met.* **95**, 191 (1983).
5. P. N. Walsh, in *Chemical Vapor Deposition*, G. G. Wadefield and J. B. Blocker, eds. (The Electrochemical Society, Pennington, NJ, 1973), p. 147.
6. R. A. Rapp, D. Wang, and T. Weisert, in *High Temperature Coatings*, M. Khobaib and R. C. Krutenat, eds. (TMS, Warrendale, PA, 1987), pp. 131–141.
7. D. M. Miller, S. D. Scarberry, and R. A. Rapp, *Oxid. Met.* **29**, 239 (1988).
8. P. A. Choquet, E. R. Naylor, and R. A. Rapp, *Mater. Sci. Eng.* **A121**, 413 (1989).

9. S. C. Kung and R. A. Rapp, *Oxid. Met.* **32**, 89 (1989).
10. D. M. Miller, PhD dissertation, The Ohio State University (1990), pp. 75–77.
11. *Binary Alloy Phase Diagrams*, Vol. 1, T. B. Massalski (ASM, Metals Park, OH, 1986), p. 104.
12. R. Bianco and R. A. Rapp, *J. Electrochem. Soc.* **140**, 1181 (1993).
13. H. Flynn, A. E. Morris and D. Carter, Proc. 25th CIM Conf. for Metallurgists, TMS-CIM, Toronto, Ontario (1986).
14. Chemical Thermodynamics of Materials, C. H. P. Lupis (Elsevier Sci. Pub. Co., NY, 1983), p. 524.
15. S. K. Gupta, S. R. Adolph, L. C. Tandon, and L. L. Seigle, *Met. Trans.* **13A**, 495 (1982).
16. S. C. Kung, Babcock & Wilcox Co., private communication.
17. P. Tomaszewicz and G. R. Wallwork, *Oxid. Met.* **20**, 75–109 (1983).
18. F. S. Pettit, *Met. Trans. AIME* **239** (1967).
19. T. Amano, S. Yajima, and Y. Saito, *Trans. Jpn. Inst. Met.* **20**, 431–441 (1979).
20. G. C. Rybicki and J. L. Smialek, *Oxid Met.* **31**, 275–304 (1989).